Mars 2020 Mobility Actuator Thermal Testing and Model Correlation

Matthew Redmond[1], Jason Kempenaar[2], and Keith Novak[3]
NASA Jet Propulsion Laboratory, California Institute of Technology, Pasadena, CA, 91109, USA

This paper describes the thermal testing and model correlation of a mobility actuator planned for use on the Mars 2020 Rover. The mobility actuator is identical to those which have been successfully flown and operated on the Mars Science Laboratory (MSL) Curiosity rover since its successful landing on Mars in August of 2012. The actuator consists of a motor, brake, and encoder paired with a four stage planetary gear box. In this thermal test, the actuator was instrumented with a number of thermocouples on both the interior and exterior of the gearbox. Heaters and a cold plate were used to generate thermal gradients across the actuator in vacuum, low pressure GN_2, and low pressure CO_2 environments in an effort to correlate a thermal model and develop a better understanding of how heat flows through the mechanism. This testing resulted in the successful model correlation of a simplified thermal model, and yielded important insights regarding the conductance of ball bearings and gear-to-gear contact. Ball bearing thermal conductance in a low pressure environment can be estimated by using correlations for vacuum thermal conductance along with a multiplier to account for increased gas conduction, and gear-to-gear conductance can be estimated by accounting for gas and grease conduction between two gears.

Nomenclature

A	=	cross sectional area	*CO₂*	=	Carbon Dioxide
A_{ins}	=	insulation cross sectional area	*DAQ*	=	Data Acquisition System
A_{metal}	=	metallic cross sectional area	*GN₂*	=	Gaseous Nitrogen
A_{tot}	=	total cross sectional area	*GSE*	=	Ground Support Equipment
ε	=	thermal emissivity	*LN₂*	=	Liquid Nitrogen
G	=	thermal conductance	*JPL*	=	Jet Propulsion Laboratory
k_{eff}	=	effective thermal conductivity	*MSL*	=	Mars Science Laboratory
k_{ins}	=	insulation thermal conductivity	*PTFE*	=	Polytetrafluoroethylene
k_{metal}	=	metallic thermal conductivity	*TC*	=	Thermocouple
k_{tot}	=	total thermal conductivity	*WSA*	=	Wheel and Steering Actuator
L	=	length			

I. Introduction

ON the Mars Science Laboratory (MSL) Curiosity Rover, thermal conductance across ball bearings was relied upon extensively to ensure that heat applied to actuator housings would be able to conduct inwards and warm up the interior mechanisms and gears of actuators before they could be operated[1]. Although bearing conductance is fairly uncertain, the bearing conductance in vacuum has been measured and shown to be a function of the bearing diameter, load, and lubrication type[2-4]. On MSL, approximate vacuum bearing conductances were used even though the actual Martian environment is low pressure CO_2. The approach of neglecting gear-to-gear contact and using vacuum bearing conductances was conservative and appropriate for use on MSL. However, this approach also resulted in long warm up durations for the MSL actuators, reducing the amount of time that could be spent performing science investigations on the surface and decreasing the operability of the MSL Curiosity Rover.

[1] Thermal Engineer, Instrument and Payload Thermal Engineering.
[2] Systems Engineer, Instrument and Payload Thermal Engineering.
[3] Principal Engineer, Spacecraft Thermal Engineering.

Detailed actuator thermal testing with temperature measurements on the actuator internals allows the thermal team to correlate a thermal model of the actuator, making the warm up predictions more accurate and less conservative. This is particularly useful on the mobility actuators, since this is the most massive actuator subsystem with a quantity of ten actuators having approximately 5.5 kg mass per actuator. With the same initial temperature, the mobility actuators use more warm up energy and take longer to warm up than any other subsystem on the Rover.

This type of a thermal test was previously requested on the MSL project, however time and funding constraints did not allow a proper test to be performed. On the MSL project, thermal testing in vacuum and low pressure environments were performed for the actuators at the sub-system and spacecraft level, however the internal actuator components were not instrumented, making it extremely challenging (if not impossible) to accurately correlate the internal components of the thermal model. This paper describes a thermal test and thermal model correlation which used internal thermocouples on a mobility actuator.

II. Test Objective

This test was designed to generate thermal data on mobility Wheel Steering Actuator (WSA) internal components which can then be used to correlate a thermal model. Two versions of the WSA were used on MSL. The WSA-1 was used for the four corner drive actuators, and the WSA-2 was used for the two mid drive actuators and the four wheel steering actuators. On the Mars 2020 rover, the WSA-2 actuator is planned for use in all 10 mobility actuator locations in order to save mass. A MSL life test WSA-2 actuator was used for this test. The WSA-2 actuator was internally and externally instrumented with thermocouples, and mounted to a thermally controlled test bracket inside a thermal vacuum chamber. Gradients were driven across the actuator using heaters mounted to the WSA-2 external housing in order to generate transient and steady state thermal data. This thermal characterization test data was used to tune the thermal conductances and capacitances in the WSA-2 thermal model. The conductance values which are of primary interest are the bearing and gear-to-gear conductance values internal to the actuator. This test was not a mechanical performance test. The WSA-2 actuator was static and was not energized at any point in the test, which is the same actuator warming condition that is used during flight.

III. Test Article Description

The WSA-2 mobility actuator which was used in this test is the MSL life test actuator. The bearings in this actuator were initially dry lubricated, since the MSL actuator design was originally intended to operate without heating down to temperatures as cold as -135 °C. However, once a decision was made to switch the MSL actuators to wet lubricated actuators, all the gearbox bearings were grease plated and then filled with some additional lubricant. All the sun gears in this actuator were also grease plated. On the first, second, and third stages of the actuator, the ring gears on the housing were lubricated directly, and the planet gears were lubricated by transfer of the ring gear grease during actuator operation. A similar, but reversed process was used on the fourth stage. On the fourth stage, the planet gears were lubricated directly, and the ring gears on the housing were lubricated by transfer of the planet gear grease during actuator operation. This lubrication approach is similar to the lubrication approach for many of the MSL and Mars 2020 actuators.

This actuator successfully passed a 2x life test on MSL over a temperature range of -70 °C to +70 °C for life testing of wet lubricated mechanisms. After passing the 2x life test, the actuator was disassembled and the motor pinion gear was re-lubricated. The actuator was then put through an additional 1x life testing at temperatures ranging from -90 °C to +30 °C in order to qualify the dry lubricated motor bearings. The colder temperature of -90 °C was used for this test to provide evidence that the actuator is capable of running colder than qualified, if necessary. In summary, on MSL, this actuator was operated for a total of 3x life, and all the grease inside of it has been operated for at least 1x life. Because the actuator had been sitting in storage for several years since last operating, the actuator was run for 1 hour both forward and backward prior to instrumenting the actuator for this thermal test. This was done to ensure the internal grease was distributed in as flight like a condition as possible.

A photograph of the WSA-2 life test unit and support bracket are shown in Figure 1. The output housing, input housing, motor, brake, and encoder are also shown in the image and were tested during the thermal test. The test bracket was designed and fabricated specifically for use in this thermal test.

The WSA-2 internal components are the primary subject of this thermal test. A cross section of the WSA-2 actuator is shown in Figure 2. The WSA-2 envelope has an outer diameter of approximately 0.12 m and a length of approximately 0.23 m. The actuator has a four stage planetary gear set, which is powered by a brushless motor. The brake is engaged by default, and will not release the rotor unless current is applied to the brake windings. The encoder, although shown only schematically in this cross section, measures the rotational position of the rotor and provides input to the flight system to control the rotational speed and positioning.

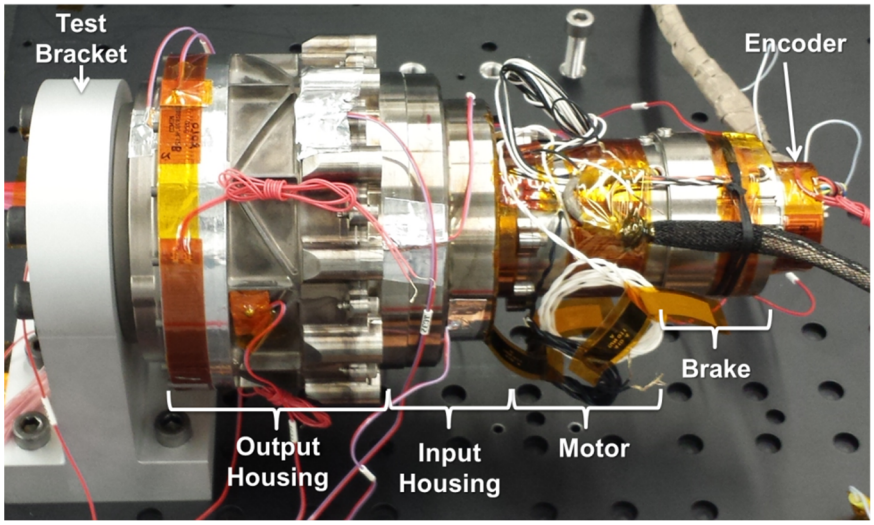

Figure 1: WSA-2 life test actuator and support bracket.

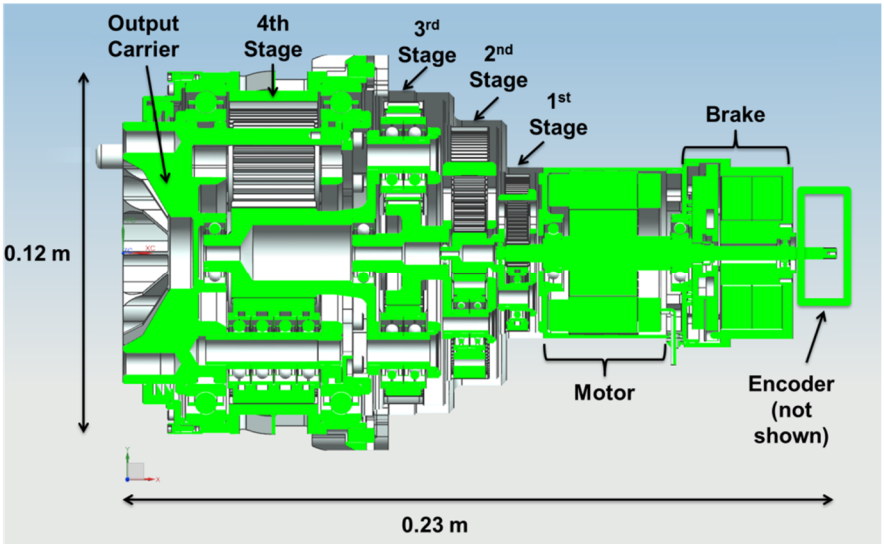

Figure 2: Cross section of the WSA-2.

The WSA-2 is made up of a large number of materials. The materials are shown in a cross section of the WSA-2 thermal model in Figure 3. The majority of the actuator is composed of stainless steel. This includes the output housing, input housing, all the planetary gears, carriers, and sun gears, and the rotor internal to the actuator. A magnet is mounted to the rotor, and the output carrier and motor housing is made of Ti-6Al-4V. The encoder housing is made of Al-7075. The brake and motor windings are predominantly copper, although they are wound around composite steel stators. A small Beryllium flange is mounted to the output housing.

The WSA-2 external surfaces were in a flight like configuration during the test. The exterior surface finishes are shown in a cross section of the WSA-2 thermal model in Figure 4. The actuator surfaces are predominantly bare metal with an assumed thermal emissivity of 0.1. The bare metal is Beryllium (Be), Titanium (Ti), or Aluminum (Al). In addition, the gearbox housing has an ion nitride stainless steel surface finish, and the brake housing is electroless nickel plated stainless steel. Kapton thin film heaters mounted to the housing have a high emissivity (ε=0.8). External test thermocouples mounted to low emissivity metallic surfaces were taped with aluminum tape to maintain a low emissivity. External test thermocouples mounted to the Kapton heaters were taped with Kapton tape to maintain a high emissivity. The thermocouples and heaters used in this test are discussed in detail in the following Section.

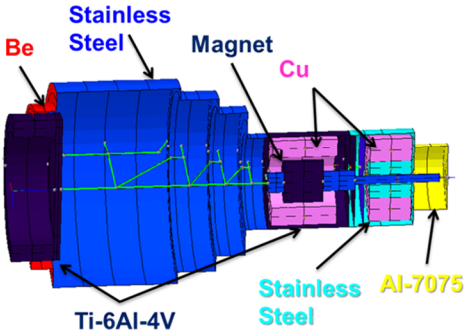

Figure 3: Cross section of the thermal model showing materials used in the WSA-2.

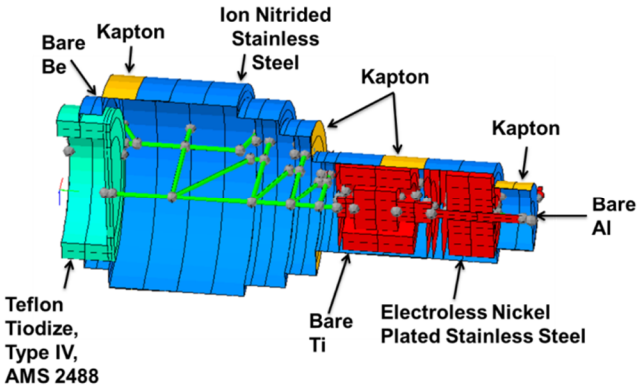

Figure 4: Cross section of the thermal model showing external surface properties of the WSA-2.

IV. Test Hardware

The test took place in a 3 foot diameter chamber in the Environmental Test Lab at JPL. The WSA-2 was mounted to a test bracket, onto a LN_2 controlled heat exchanger and magnesium adapter plate, as shown in Figure 5. This mounting configuration ensures that the heat dissipated on the actuator housing is forced to flow through the internal gears and bearings of the actuator to the cold output carrier and mounting bracket. This heat flow produces gradients that are larger than the temperature measurement uncertainty and allowed the thermal model to be correlated. A horizontal configuration was desired so that the potential effects of any settling of the internal gears, carriers, and grease within the actuator could be observed and noted. On Mars, the six drive actuators will be in an approximately horizontal configuration, just like the test actuator. The four wheel steering actuators will be in a vertical configuration in flight. The output carrier and output bearings, not the gears, are preloaded and carry the weight of the rover during surface operations. The bearing preload was maintained in the flight like condition for this test.

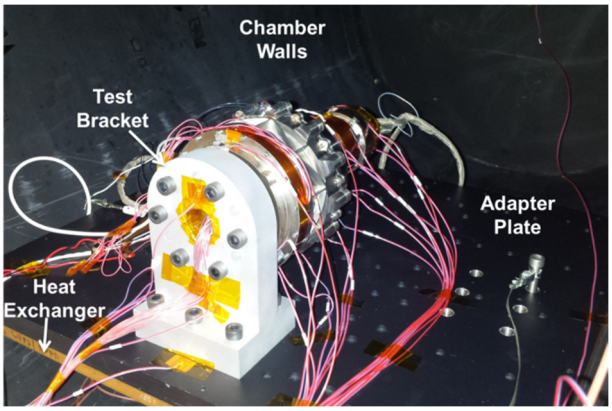

Figure 5: Test configuration with test bracket, adapter plate, heat exchanger, and 3 foot chamber.

There are a total of 6 Kapton film test heater elements on the WSA-2, located in 4 regions, and controlled using 3 power supplies. The test heater locations are shown in Figure 6, and close up images of the installed heaters are shown in Figure 7. The three output heaters had measured resistances of 76.5, 76.2, and 77.0 Ω, and the encoder heater had a measured resistance of 82.9 Ω. The input housing (flange) heater had a measured resistance of 52.2 Ω, and the motor (side) heater had a measured resistance of 107.2 Ω.

The power supplies used for this test were Agilent N6700 power supplies. The actual resistance of each circuit was 0.3 to 0.4 Ω higher than expected if the measured heater resistance alone is taken into account. This additional resistance is attributed to the resistance in the wire leads and chamber feed-throughs.

A total of three pressure sensors were used during this test: an ion gage, a convectron gage, and a baratron gage. Although all three pressure gages read similar values, the ion gage is most accurate for vacuum conditions, the convectron gage is most accurate for low pressure (~ 6 torr) N2, and the baratron gage is most accurate for low

pressure (~ 6 torr) CO2. The data acquisition system was used to record all test data (voltage, current, temperature, power, and pressure) at 1 minute intervals during the test. All pressure data was also recorded hourly by hand.

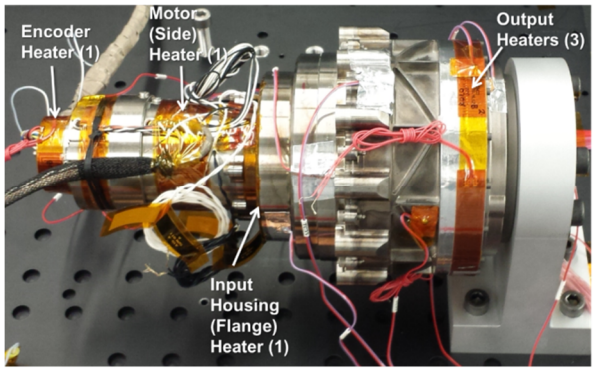

Figure 6: Test Heater Locations.

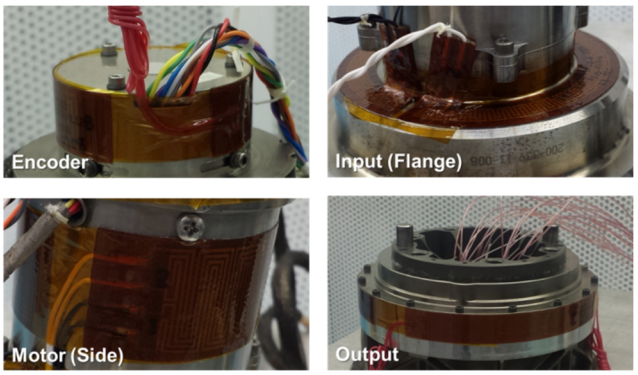

Figure 7: Close Up of Test Heater Locations.

All thermocouples used in this test were Type E thermocouples (TCs). Internal TCs were 6 ft long, 36-gage Omega TCs with Teflon insulation and were numbered 1 to 24. It should be noted that TCs 1 and 2 were not installed due to a lack of space, and TC 6 fell off during the bonding process and was not reapplied due to schedule constraints. External TCs were 6 ft long, 26 gage, JPL made TCs with copper tabs and were numbered 25 to 60.

The internal TCs were spread out among the 4 stages of the WSA-2. If TCs 1, 2, and 6 had been installed on the first stage, then each stage would have had 2 planet gear TCs, 2 carrier TCs, and 2 sun gear TCs. These thermocouple locations were chosen to match the node locations in the WSA-2 reduced node thermal model. This helped to reduce the effort required to correlate the thermal model. For every stage, to the extent possible, one of the instrumented planet gears was assembled such that the planet was touching the bottom face of the actuator housing. This caused that planet to bear the weight of the carrier and other planets in that stage. The other instrumented planet was then as close to 180° away as possible, meaning that it had a minimal amount of loaded weight. Ultimately, no significant difference was observed between the bottom and top temperatures, which indicates that these gravity effects were not significant.

The test error caused by introducing TCs, which serve as additional heat flow paths in the actuator, is shown to be insignificant. The cross section of the 36 gage TCs was measured to be 0.031" x 0.018". The effective kA of 36 gage type E TC wire = $k_{tot}A_{tot} = k_{metal}A_{metal} + k_{ins}A_{ins} = 8.4 \times 10^{-7}$ W-m/K. The minimum clearances in regions where TCs were installed is 1.5 mm, so the worst case shorting conductance, G = kA/L = 0.00056 W/K, which is only 16% of even the smallest sun to planet gear-to-gear conductances estimated during this test. Most likely, any thermal shorts caused by TC wire would not occur along the shortest path between two components. An infinite fin approach can be used to estimate TC wire heat losses and results in a conductance of G = 0.0002 W/K, which is even smaller.

A cross section showing the approximate interior and exterior actuator TC locations of an assembled actuator is contained in Figure 8. Thermocouple placement on the mounting bracket, heat exchanger plate, shroud, and a floating thermocouple to measure chamber ambient gas temperature is shown in Figure 9. The WSA-2 actuator was unpowered and non-operational for the duration of this test. Carrier TCs were placed on the carrier so that they were near to the instrumented planet gears. The planet gears were instrumented with TCs so that the TCs would measure the planet gear temperature away from the housing and sun gear. In addition, external TCs mounted to the actuator housing matched the locations of the instrumented planets of each stage, to the extent possible, in order to more directly measure the temperature difference between the planet gear and housing. External TCs which were not on one of the 4 stages were mounted 180° apart, one on the top and one on the bottom. The exact TC locations on the internal actuator components was not determined until after the initial actuator disassembly and TC installation, due to the complexity of the actuator internals. The installation was a painstaking process which required feeding TC wire through planetary gear stages and vent holes located on output carrier of the WSA-2. These vent holes which were used for TC access are shown in Figure 10. As many as 8 TC wires were routed through a single vent hole.

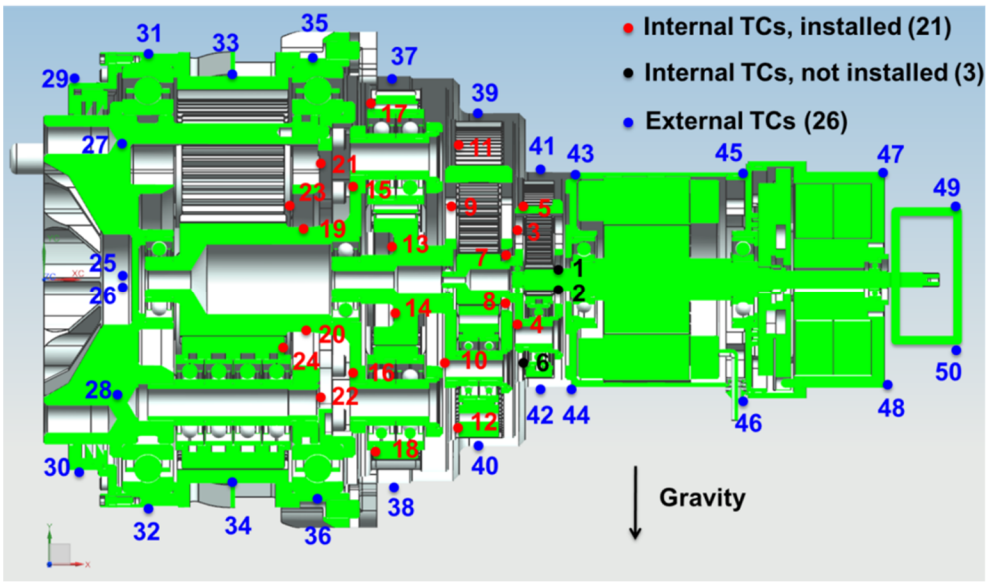

Figure 8: Approximate TC placement on the on the interior and exterior of the WSA-2.

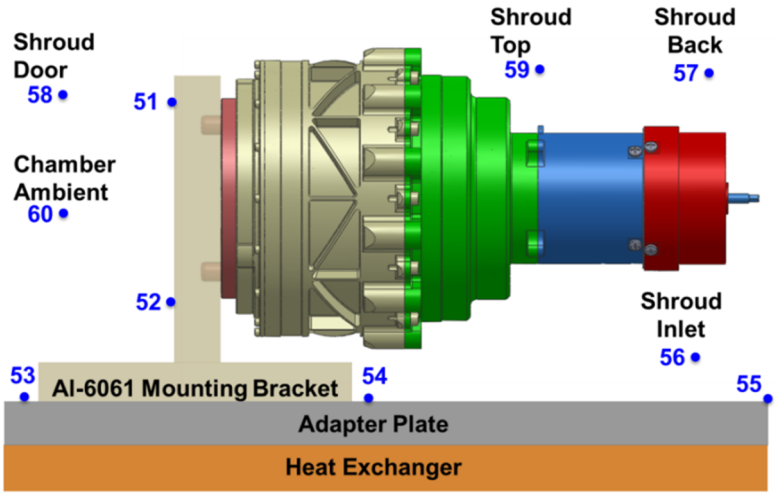

Figure 9: TC placement on the mounting bracket, heat exchanger, and shroud.

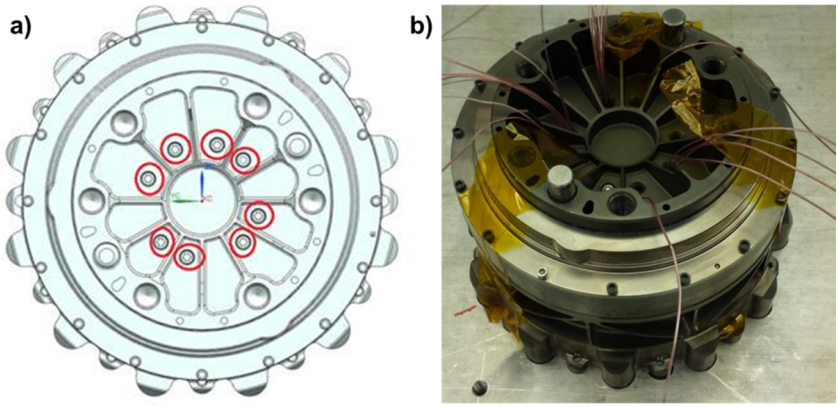

Figure 10: Vent holes used for TC Access. a) schematic showing vent holes, b) instrumented actuator with TC wires routed through the vent holes. The TC wires do not excessively block vent holes.

V. Test Matrix

The As-Run Thermal Test Matrix for this test is shown in Table 1. The test can broadly be broken up into four sections. First, vacuum testing was performed with a -100 °C shroud and heat exchanger. Performing vacuum testing first ensured that all moisture was removed from the chamber. Vacuum testing was followed by 6 torr N_2 testing with a -100 °C shroud and heat exchanger. Testing in a 6 torr N_2 environment was performed because it is not possible to maintain low CO_2 pressure at such cold shroud and heat exchanger temperatures. CO_2 has been known to freeze out of the environment onto the shroud or heat exchanger LN_2 inlet. Both Vacuum and 6 torr N_2 testing have three parts: output only heating, input only heating, and combined heating, which all produce different combinations of thermal gradients within the actuator to help correlate the thermal model. A third test section, which included elevated temperature testing in 6 torr N_2 and 6 torr CO_2 environments with the shroud and heat exchanger at -20 °C, was also performed. This testing was more limited in scope, with only the input heating being performed for each environment. The prescribed heating was reduced for this portion of the test to avoid overheating the test article. The third test section verified our ability to convert conductance values obtained in a N_2 atmosphere to those which would occur in a CO_2 atmosphere, due to the differing thermal conductivity of the gases. Finally, the test article was heated up to ambient temperatures. This was done using a shroud and heat exchanger temperature setpoint of 30 °C. The test was completed once all test hardware was above room temperature (20 °C), and the chamber was opened. Steady state for this test took about 13 hours to reach for the vacuum cases, and 8 to 11 hours for the gas environment cases. The steady state criteria was defined as when all the TCs change by no more than 0.2 °C in 1 hour.

Table 1: As-Run Test Matrix. Heater powers > 0 W are shown in red.

Test Number	Description	Pressure	Atmosphere	Shroud Temperature	Heat Exchanger Temperature	Output Power	Input Flange Power	Input Motor Power	Encoder Power	Total Power
		(Torr)		(C)	(C)	(W)	(W)	(W)	(W)	(W)
1.0	Pump Down	760 torr to 1e-5 torr	Air	Floating	Floating	0.0	0.0	0.0	0.0	0.0
1.1	Cool Down, Vacuum	< 1.0 e -5	Vacuum	-100	-100	0.0	0.0	0.0	0.0	0.0
1.2	Output Heater Warm Up, Vacuum	< 1.0 e -5	Vacuum	-100	-100	**22.0**	0.0	0.0	0.0	**22.0**
1.3	Cool Down, Vacuum	< 1.0 e -5	Vacuum	-100	-100	0.0	0.0	0.0	0.0	0.0
1.4	Input Heater Warm Up, Vacuum	< 1.0 e -5	Vacuum	-100	-100	0.0	**6.6**	**3.2**	**3.2**	**13.0**
1.5	Cool Down, Vacuum	< 1.0 e -5	Vacuum	-100	-100	0.0	0.0	0.0	0.0	0.0
1.6	Combined Heater Warm Up, Vacuum	< 1.0 e -5	Vacuum	-100	-100	**11.0**	**3.3**	**1.6**	**1.6**	**17.5**
1.7	Cool Down, Vacuum	< 1.0 e -5	Vacuum	-100	-100	0.0	0.0	0.0	0.0	0.0
2.0	Vacuum to N_2 Transition	6 +/- 1	N_2	-100	-100	0.0	0.0	0.0	0.0	0.0
2.1	Output Heater Warm Up, N_2	6 +/- 1	N_2	-100	-100	**22.0**	0.0	0.0	0.0	**22.0**
2.2	Cool Down, N_2	6 +/- 1	N_2	-100	-100	0.0	0.0	0.0	0.0	0.0
2.3	Input Heater Warm Up, N_2	6 +/- 1	N_2	-100	-100	0.0	**6.6**	**3.2**	**3.2**	**13.0**
2.4	Cool Down, N_2	6 +/- 1	N_2	-100	-100	0.0	0.0	0.0	0.0	0.0
2.5	Combined Heater Warm Up, N_2	6 +/- 1	N_2	-100	-100	**11.0**	**3.3**	**1.6**	**1.6**	**17.5**
3.0	Heat Exchanger and Shroud Transition, N_2	6 +/- 1	N_2	-20	-20	0.0	0.0	0.0	0.0	0.0
3.1	Soak to Steady State, N_2	6 +/- 1	N_2	-20	-20	0.0	0.0	0.0	0.0	0.0
3.2	Input Heater Warm Up, N_2	6 +/- 1	N_2	-20	-20	0.0	**3.3**	**1.6**	**1.6**	**6.5**
3.3	Cool Down, N_2	6 +/- 1	N_2	-20	-20	0.0	0.0	0.0	0.0	0.0
3.4	Transition to CO_2	6 +/- 1	CO_2	-20	-20	0.0	0.0	0.0	0.0	0.0
3.5	Input Heater Warm Up, CO_2	6 +/- 1	CO_2	-20	-20	0.0	**3.3**	**1.6**	**1.6**	**6.5**
3.6	Cool Down, CO_2	6 +/- 1	CO_2	-20	-20	0.0	0.0	0.0	0.0	0.0
4.0	Return to Ambient	6 +/- 1	CO_2	30	30	0.0	0.0	0.0	0.0	0.0
4.1	Chamber Break	6 +/- 1	CO_2	30	30	0.0	0.0	0.0	0.0	0.0

VI. Post Test Inspection and Disassembly

During the actuator disassembly and removal of the thermocouples, a wrench was used to break the adhesive bond and open up the actuator. During this process, the output half of the actuator was violently turned about 30 degrees relative to the input half of the actuator. The output half of the actuator was slowly lifted and it was clear that a number of the TCs had debonded. It is unknown whether the TCs debonded during the test or during disassembly. The actuator stages were disassembled one by one, and careful attention was given to record which TCs remained bonded through the entire test and disassembly process. The status of each internal TC and location for the duration of the test is listed in Table 2.

Table 2: Status of each internal TC and location for the duration of the test

Description	Top TC		Bottom TC	
	TC Number	Status	TC Number	Status
1st Stage Sun	1	Not Installed	2	Not Installed
1st Stage Carrier	3	Debonded	4	Did Not Debond
1st Stage Planet	5	Debonded	6	Not Installed
2nd Stage Sun	7	Debonded	8	Did Not Debond
2nd Stage Carrier	9	Debonded	10	Debonded
2nd Stage Planet	11	Debonded	12	Debonded
3rd Stage Sun	13	Did Not Debond	14	Debonded
3rd Stage Carrier	15	Did Not Debond	16	Did Not Debond
3rd Stage Planet	17	Did Not Debond	18	Did Not Debond
4th Stage Sun	19	Debonded	20	Debonded
4th Stage Carrier	21	Did Not Debond	22	Did Not Debond
4th Stage Planet	23	Debonded	24	Debonded

Table 2 highlights that 24 internal thermocouples were intended to record temperatures for 12 physical locations inside the actuator. At 6 of the 12 locations, at least 1 thermocouple remained installed for the duration of the test and disassembly. At 5 of the 12 locations, it is not known whether the thermocouples remained installed for the duration of the test, since no thermocouples remained bonded after disassembly. At 1 of the 12 locations, thermocouples were not installed.

Although it is not possible to know for sure when the debonding occurred, it is likely that the debonding occurred during disassembly. The reason is that at the 1st Stage Carrier, 2nd Stage Sun, and 3rd Stage Sun TC locations, one TC remained bonded after disassembly and one TC did not remain bonded after disassembly. In the test data, these TCs remained within 2 °C of one another for the duration of the test. In addition, many of the TC locations where both TCs debonded also recorded temperatures with 2 °C of one another for the duration of the test. It is likely that if these TCs had debonded during the test, a temperature difference of greater than 2 °C would have been recorded on at least one of them. As a result, test data from all TCs (bonded and de-bonded) were used in model correlation.

VII. Test Results

Overall, the test went very well. The test began on May 10th , 2016 at 9:50 am and was completed on May 19th, 2016 at 8:30 am. No temperature alarm limits were exceeded, and the test was completed on schedule.

The chamber pressure, as measured by the ion gage, for the duration of the test is shown in Figure 11. The pressure was well below 1x10^{-5} torr for the vacuum portion of the test. For the N_2 and CO_2 portions of the test, the pressure remained at 6 +/- 1 torr. It was necessary to pump some of the gas out when the shroud and heat exchanger transitioned from -100 °C to -20 °C. A pump down also was used to transition the chamber from GN_2 to CO_2. These pressure effects are visible in Figure 11.

The bracket, shroud, and ambient temperatures for the duration of the test are shown in Figure 12. The heat exchanger and bracket both had two TCs. Temperatures shown in Figure 12 are averages for these components. A rise and fall of the heat exchanger and bracket temperature can be seen as the heater power is turned on and off. The chamber ambient is measured using a TC covered in Aluminum tape, and is only physically meaningful for the GN_2 and CO_2 test cases. The shroud door thermocouple was attached to a sheet of aluminum foil. The aluminum foil sheet was stretched across the uncontrolled door of the chamber, which is why its temperature is relatively high throughout the test. However, the aluminum test bracket is the only part of the actuator which had a good view to the low emissivity foil, so it did not have a significant effect on the test. The TC on the back part of the shroud appeared to be located at a cold spot on the shroud. As a result, the TC on the top part of the shroud is used for the thermal model correlation to represent shroud temperature.

The as-run heater power profile is shown in Figure 13. The heater powers of each circuit were measured by the data acquisition system. Minor adjustments to the as measured heater power was made to account for the power dissipated in the chamber feed throughs so that the values shown in Figure 13 only include the power dissipated at the heater patch itself.

One of the key features of this test was that all the actuator TCs were redundant. One of the reasons this was done was to determine if there was any difference between the gear-to-gear contact on the top or bottom gears. As a result, the temperature difference between the bottom and top TCs were compared. The temperature difference (Bottom – Top) for any TC which had more than 2 °C of difference during the test is shown in Figure 14. A few trends were observed:

1. The 1st Stage Carrier, 2nd Stage Sun, and 3rd Stage Sun TC temperature differences were within 2 °C for the duration of the test. This is extremely relevant to all the collected data because at all three locations there was one TC which remained bonded after disassembly and one TC which did not remain bonded. In addition, many of the TC locations where both TCs debonded also recorded temperatures with 2 °C of one another for the duration of the test. It is likely that if these TCs had de-bonded during the test, a temperature difference of greater than 2 °C would have been recorded.
2. Second, none of the TCs had temperature differences greater than 2 °C during the GN_2 or CO_2 portions of the test. This suggests that temperatures will likely be symmetric in the gaseous Martian environment. However, all of the planet TCs which were redundant (the first stage planet only ended up having 1 TC installed), did have periods of time with a significant temperature difference during the vacuum portion of the test. This could have been caused by varying orientation and thermal contact between gear teeth. In a vacuum, such variations in thermal contact are expected to cause more pronounced temperature differences than in a gas, which can fill in gaps and make thermal conductance across gear teeth less sensitive to individual planet orientation. These variations in gear-to-gear conductance do not seem to be explained by gravity effects since there is not a consistent pattern of the bottom planet gear warming faster than the top planet gear.
3. Third, the temperature difference between the top and bottom 4th stage housing was likely caused by a loose 4th stage bottom housing TC. This explains why the bottom TC was sometimes colder than the top TC, if only by 3 °C at the most, but the bottom TC was never warmer than the top TC. This TC was confirmed to be loose during the post-test inspection.
4. Fourth and finally, there was a significant temperature difference between the top and bottom encoder temperatures. One possible cause is that the bolts used to attach the encoder to the brake did not produce even contact. The encoder used in this test was not the same one used for the WSA-2 life test, but was a spare encoder installed just to allow the gearbox to operate for 1 hour in both directions and ensure that the grease in the gearbox was in a flight like state. As a result, the encoder was not installed with as much care as would be done for flight implementation.

Due to the close matching of the redundant TCs, especially in a gaseous environment, the remainder of this paper only reports the average temperature of both redundant TCs. Furthermore, the model correlation is done using only the average temperature of redundant TCs.

The actuator gear box temperatures are shown in Figure 15. This plot shows that the temperatures of a single actuator stage tend to track one another fairly well, and that the primary gradients in the actuator for the test configuration are axial, and not radial. This suggests that the radial conductance via gear to gear contact is better than anticipated. The input side of the gear box is warmer with input only heating, and the output side of the gear box is warmer with output only heating. The maximum gradient within each actuator stage is shown in Figure 16. Gradients are largest on the input side of the actuator when input only heating is used, and gradients are largest on the output side of the actuator when output only heating is used. Finally, actuator brake and encoder temperatures are shown in Figure 17. There is a significant axial gradient in the encoder, brake, and motor housing.

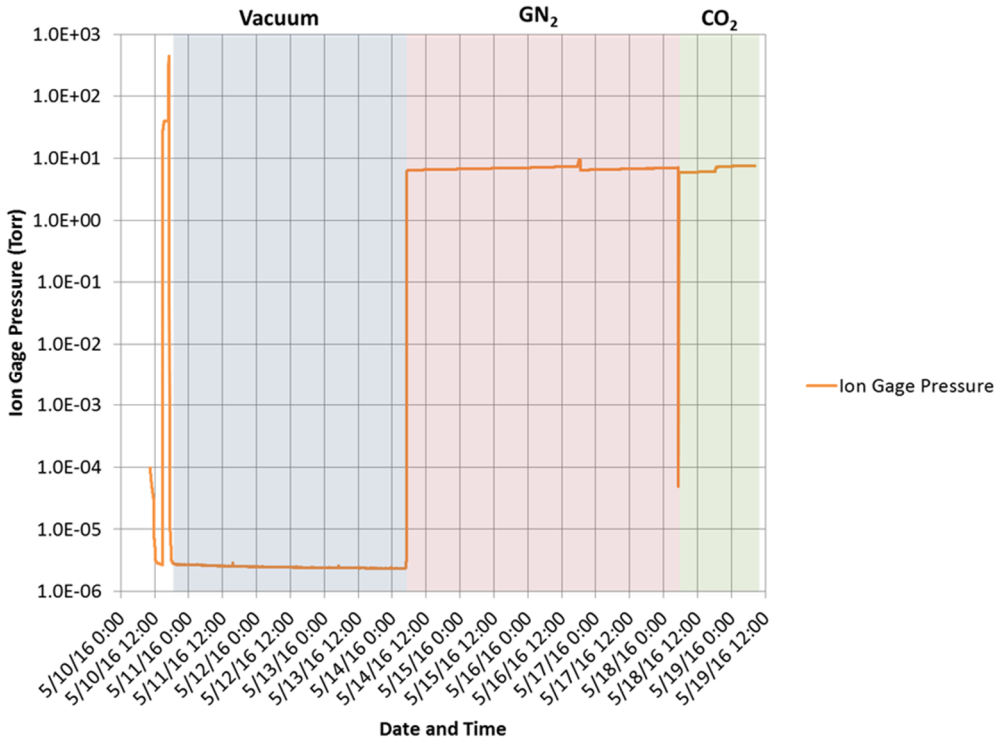

Figure 11: Chamber pressure for the duration of the test.

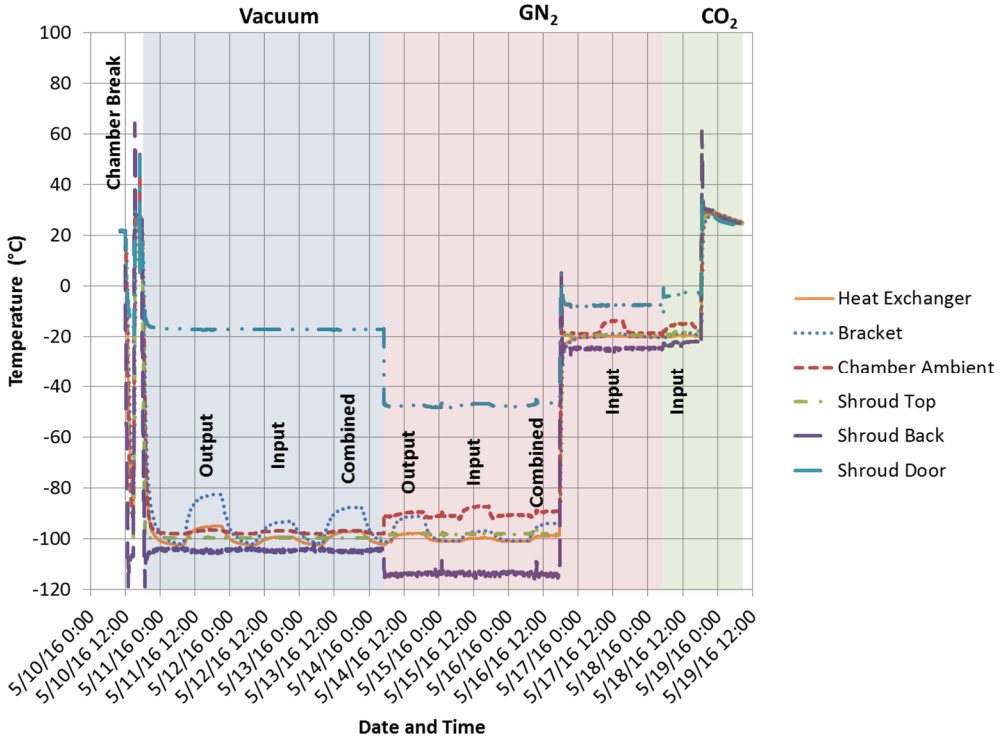

Figure 12: GSE, shroud, and ambient temperatures for the duration of the test.

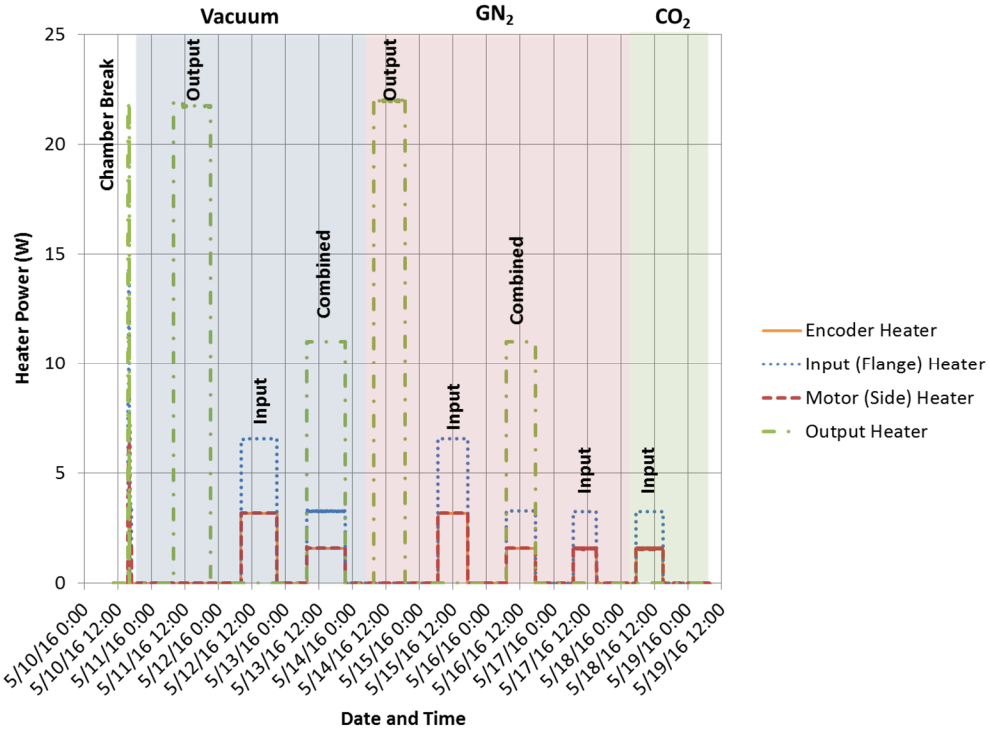

Figure 13: As-Run Heater Power Profile.

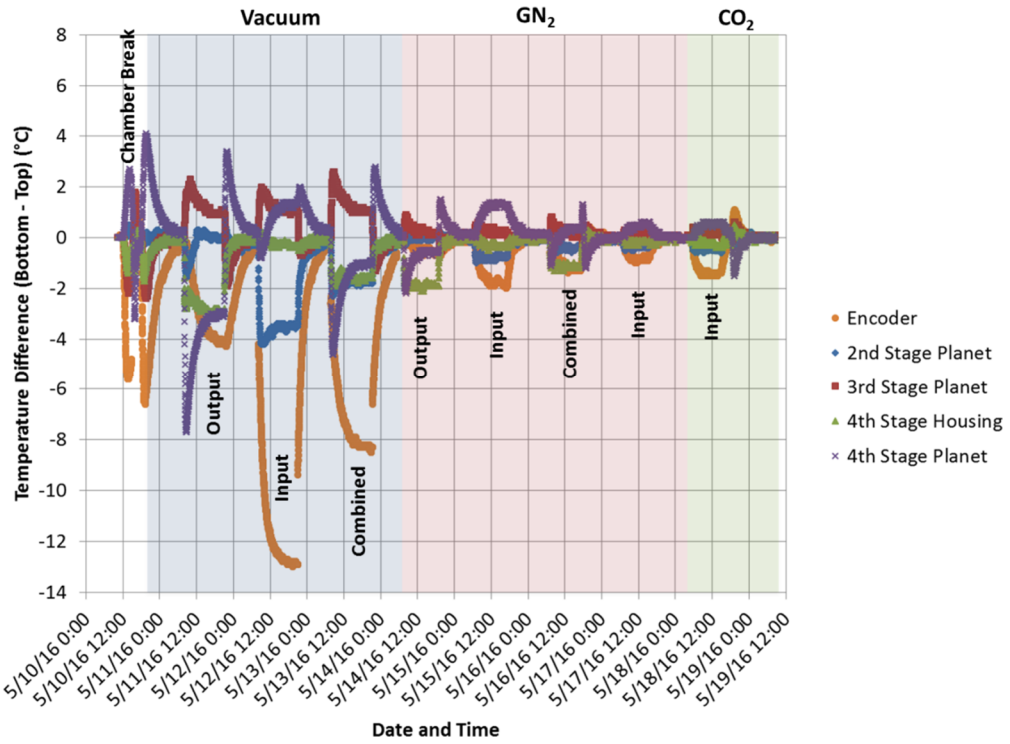

Figure 14: Temperature difference between top and bottom TCs which exceeded 2 °C at some point during the test. All of the temperature differences greater than 2 °C occurred during the vacuum portion of the test.

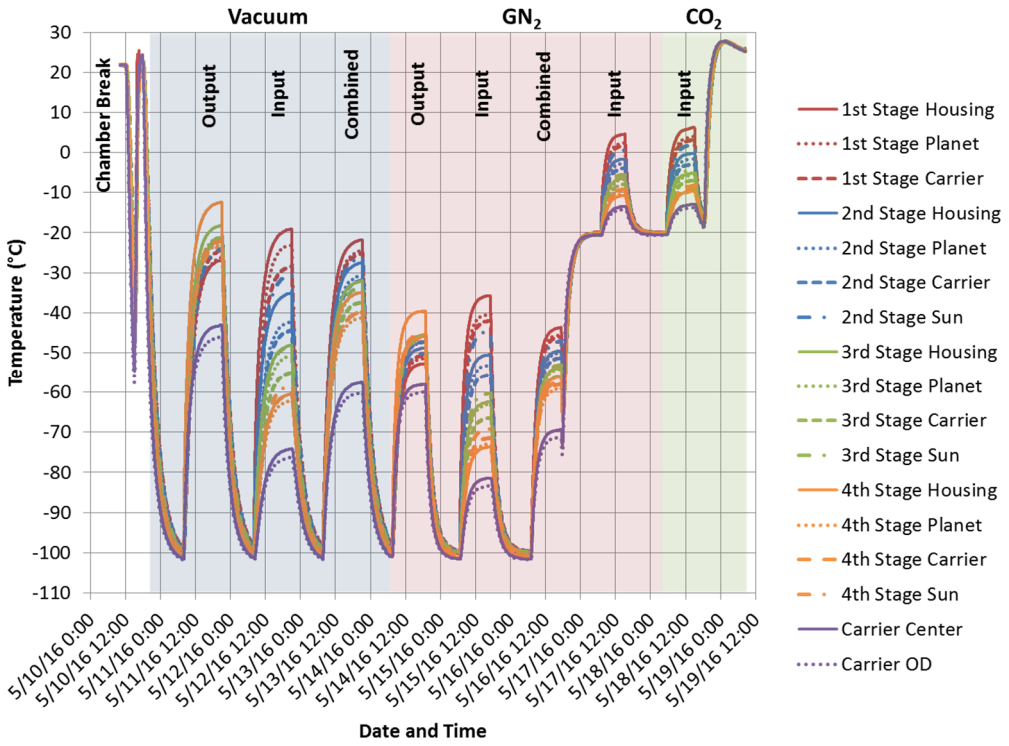

Figure 15: Actuator gear box internal and external temperatures. The average temperatures of redundant TCs are shown due to the close matching (within 2 °C) of redundant TCs, especially in the gas environment testing.

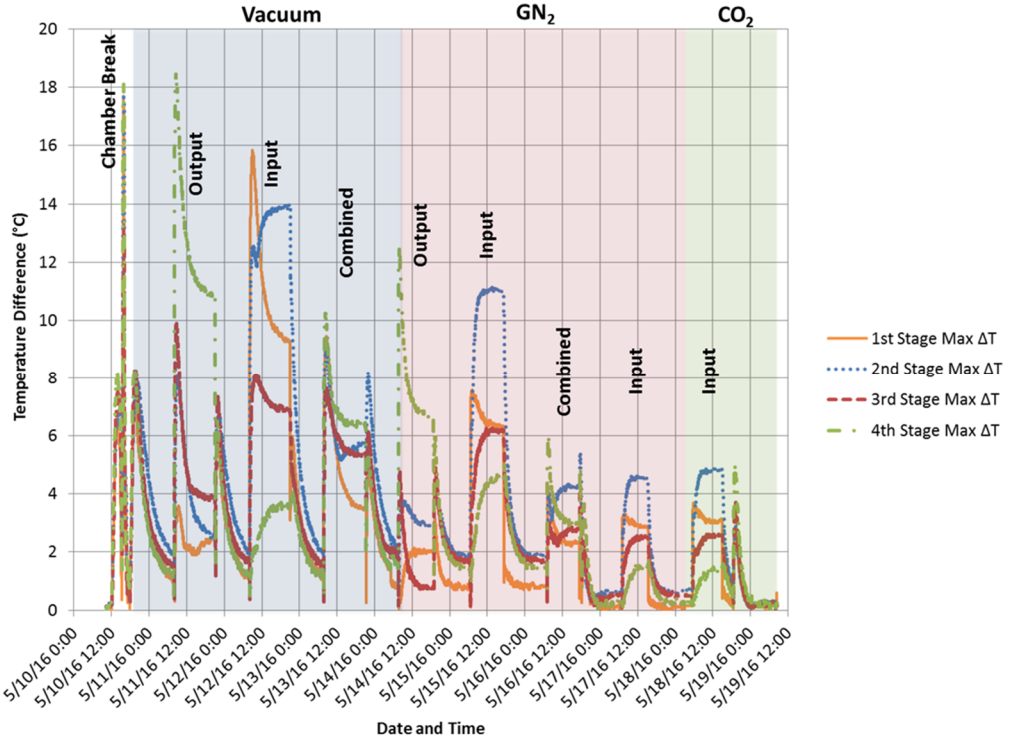

Figure 16: The maximum gradient within each actuator stage. The average temperatures of redundant TCs are shown due to the close matching (within 2 °C) of redundant TCs, especially in the gas environment testing.

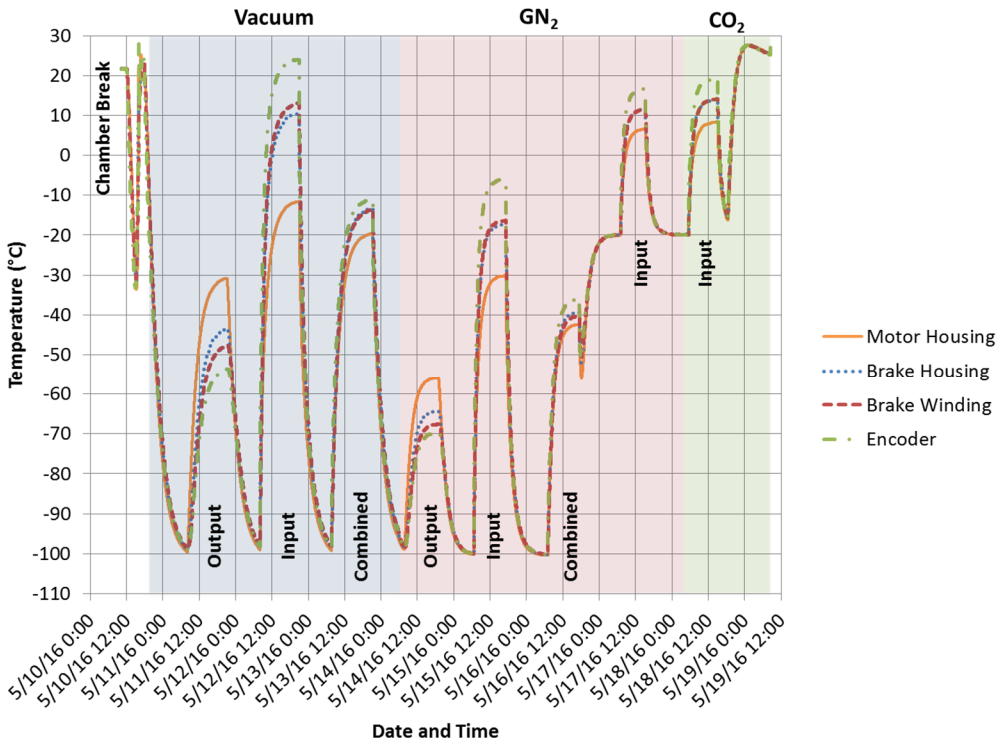

Figure 17: Actuator brake and encoder temperatures. The average temperatures of redundant TCs are shown due to the close matching (within 2 °C) of redundant TCs, especially in the gas environment testing.

VIII. Thermal Model Correlation

A. Initial Model

A simplified WSA-2 thermal model was built in Thermal Desktop® to help in the planning and preparation for this test. This simplified model was also correlated using thermal data from this test and used to generate flight predictions. The simplified model is axisymmetric, and uses non-geometric nodes to simplify the complex internal 4-stage planetary gear train in the WSA-2 actuator. Each node in the thermal model has a corresponding internally instrumented TC in order to aid model correlation. The non-geometric nodes are numbered such that the first digit stands for the gear stage, and the 2nd digit stands for sun gear (0), planet gear (1), or carrier (2). One exception is on the 4th stage output carrier where there are two carrier nodes. This simplified model and numbering scheme is shown in Figure 18.

The key assumptions in this thermal model are the conductance values for bearings, gear-to-gear contact, and carriers. All the WSA-2 bearings were wet lubricated with Braycote 601, except for the Input Rotor Bearings which were dry lubricated. Bearing conductance values are estimated for marginally lubricated bearings in a vacuum, or for bearings with no lubrication, based off the guidance in literature[4]. For bearing conductance in an atmosphere, a multiplier of 3 is assumed as a lower bound since bearings have 3 to 10 times greater conductance in atmosphere than in a vacuum[4].

The assumed gear-to-gear contact conductance is based off an A/L of the gear-to-gear interface. This is an approximate term which was measured using the WSA-2 solids model using the method shown in Figure 19. In this method, the gear-to-gear conductance, $G = k_{eff}*A/L$, where A is the produce of chord width and planet width and L is the upper bound gas gap. The effective thermal conductivity (k_{eff}) across the gap depends on the gas species, gas temperature, and how much grease is present across the gear-to-gear interface. The initial model for the test profile assumed $k_{eff} = 0$ in a vacuum, and $k_{eff} = 0.02$ W/m-K in the low temperature N_2 cycles, $k_{eff} = 0.025$ W/m-K in the high temperature N_2 cycles, and $k_{eff} = 0.015$ W/m-K in the high temperature CO_2 cycles. These numbers were chosen based off of an approximate temperature dependent thermal conductivity during each part of the test.

Finally, carrier-to-sun-gear conductances (via pure conduction through stainless steel) were obtained in a finite element analysis of the carrier solids models.

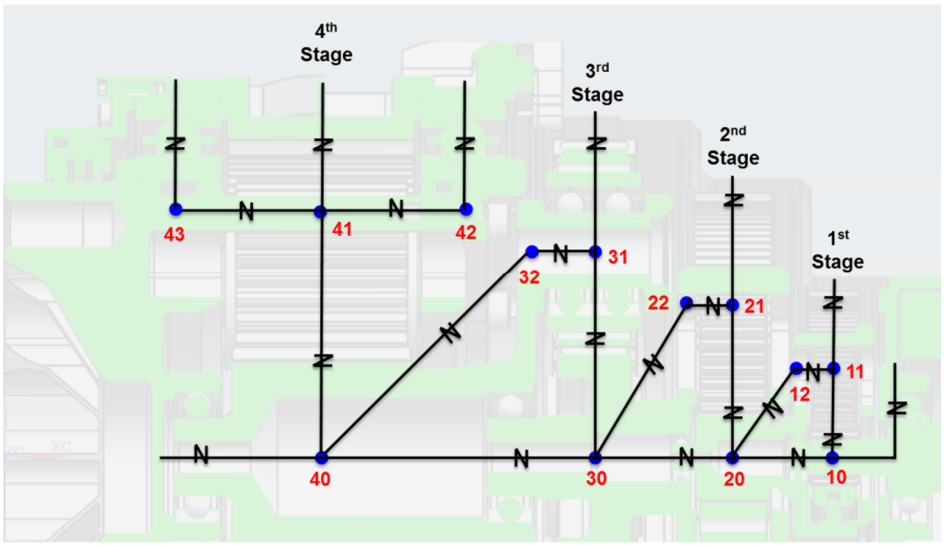

Figure 18: Simplified thermal model and node numbering scheme. The first digit corresponds to the 1st, 2nd, 3rd, and 4th stages. The second digit indicates whether the node is a sun gear (0), planet gear (1), or carrier (2).

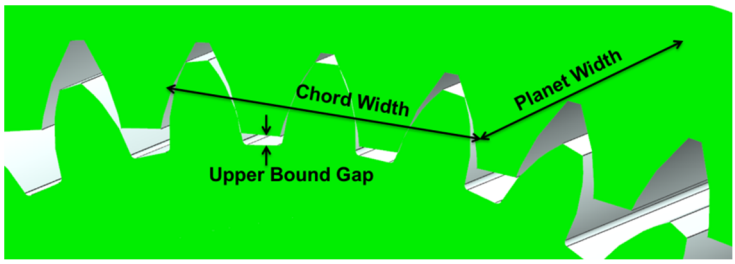

Figure 19: Method used to estimate the A/L for the gear-to-gear interface.

B. Model Correlation

During thermal model correlation, a few principles were used to ensure that the resulting model correlation was useful as a predictive model for Mars surface operations. First, care was taken to ensure that all model changes were physically meaningful. Second, the model correlation of the gear box and gear box internals was prioritized over the model correlation of the brake, motor, and encoder. Third, correlation of the gear-to-gear contact and bearing conductance was done so that the results could be generalized to other actuators, as much as possible. Fourth, the correlation was performed to ensure that the model remained slightly conservative.

Although the correlation was ultimately iterative, the general approach was to first make improvements which resulted in a more accurate prediction of actuator housing temperatures, and then make changes in the gear-to-gear and bearing conductance assumptions. Both bearing and gear-to-gear conductances were changed using multipliers. In this way, all of the bearing conductances were scaled by the same value. It was found that the bearing conductances did not need to be changed from the initially guessed values based on the published correlations[4]. Gear-to-gear conductance values also were scaled by a single value, based on their A/L as measured using the method shown in Figure 19. This approach is believed to result in bearing and gear-to-gear conductance values are generalizable and physically meaningful.

The correlation efforts were also made with the intent that the model should be conservative, even after model correlation. For actuator warm up, lower conductance values result in models which predict more energy and time needed to warm the actuator. As a result, efforts were made to have an actuator housing which was biased slightly warm during warm ups, as well as internal components that were biased slightly cold. Having modeled gradients slightly larger than test gradients ensures some element of conservatism.

Two methods were used to evaluate the accuracy of the model predictions against the test data and correlate the model. First, graphing of the model results against the test data allowed visual comparison, which was very useful in determining trends and in finding discrepancies in the model. However, a numerical measure of model accuracy was also used. The average absolute error between the model and the test data served as a good numerical metric for model accuracy. The average absolute error of all test data for the duration of the test was 5.77 °C using the initial

model, and 2.80 °C using the final correlated model. It should be noted that further reductions in the average absolute error were possible, however such changes were not made because they would have resulted in a loss of model conservatism or physical realism.

The changes made during model correlation can be summarized into five broad categories:

1) Changes made to improve the motor/brake/encoder part of the model. This part of the model had the most error, but was also the lowest priority due to its low mass.
2) Changes made to improve the gearbox temperature predictions. This part of the model required only a few changes, but is the most critical part of this thermal model.
3) Changes made which affected both the motor/brake/encoder, as well as the gearbox.
4) Changes to bearing conductance. A sensitivity study on the bearing conductance indicated that no changes were needed to the assumed conductance values.
5) Changes to the gear-to-gear conductance assumptions. These changes are important since they were the primary motivation for performing this test.

1) Changes to improve the motor/brake/encoder model

- The brake and motor winding bond contactors were changed to conductors. The high conductance contactors were introducing an artificial thermal short into the model. Of all the model changes made to correlate the motor/brake/encoder, this change was the most significant.
- The convection coefficient on the motor/brake/encoder side of the actuator was increased to account for the smaller diameter of this part relative to the gearbox.
- A conductivity multiplier of 0.5 was used on the titanium motor housing. This multiplier accounts for heat spreading at the bolted joint interface between the motor housing and brake housing. Hand calculations indicate that the thermal conductance due to heat spreading in the thin walled housing is almost the same as the axial conductance of the motor housing, which is why using a multiplier as low as 0.5 is justified.
- A conductivity multiplier of 0.8 was used on the brake housing. This 20% decrease in conductance on the housing is within the margin of error which would be expected from the model, and is justified by considering the effect of heat spreading from bolted joints. This change significantly improved the correlation of the thermal model to the test data.
- A cabling heat loss term was added from the encoder to the ambient.

2) Changes to improve the gearbox model

- The nodalization of the output carrier was changed so that the TC measurement locations were better aligned with the nodal location in the thermal model. This significantly improved the model correlation on the output carrier.
- A conductivity multiplier of 0.8 was used on the entire actuator gearbox housing. This 20% decrease in conductance on the housing is within the margin of error which would be expected from the model, since the housing surfaces were approximations of complex solid machined parts. This change significantly improved the correlation of the thermal model to the test data.

3) Changes to improve both the motor/brake/encoder and gearbox models

- An extra node on the motor housing was added so that the motor (side) heater power could be applied to the correct location. This resulted in a better model correlation for both the motor/brake/encoder as well as the gearbox.
- A mass multiplier of 0.5 was applied to the motor and brake copper windings. This change was made since the motor/brake/encoder part of the model was lagging in temperature compared to the test data. A more detailed investigation into the mass breakdown indicated that the motor/break/encoder mass was overestimated in the initial thermal model. This change is physically realistic because the motor and brake windings are not truly 100% volume fraction copper, as they were previously assumed. This mass was re-assigned to the gearbox by applying a mass multiplier of 1.1 to the entire gearbox. The new model mass is 5.54 kg, which is within 1% of the measured actuator mass on the MSL project. This new mass breakdown is believed to be both more accurate and more conservative because it places more mass on the region which must be warmed up and less mass on the less critical parts of the hardware.

4) Changes to bearing conductance

The initially assumed bearing conductance values in vacuum and atmosphere were not changed during the model correlation. Bearing conductance values were estimated for marginally lubricated bearings in a vacuum, or for bearings with no lubrication, and are based off the guidance in literature[4]. For bearing conductance in an atmosphere, a multiplier of 3 was assumed as a lower bound since bearings have 3 to 10 times greater conductance in atmosphere than in a vacuum, as described in literature[4]. This assumption seemed reasonable since gas conduction is independent of pressure at macroscopic length scales, even though previous bearing conductance data was taken in ~760 torr (1 atm) air, not the ~ 6 to 10 torr CO_2 which is present on the Martian surface.

A bearing conductance sensitivity study was performed to verify the assumed bearing conductances in the thermal model. Bearing conductances are changed by +/- 50% for this study. First, a multiplier was used to change the bearing conductance during the vacuum portion of the test, leaving all other parts of the model constant, as shown in Figure 20. Next, a multiplier was used to change the bearing conductance during the atmospheric portion of the test, leaving all other parts of the model constant, as shown in Figure 21. The average absolute error between the model and the test data was used to understand how these changes affect model accuracy using four groups of TCs. First, all the actuator TCs were used. Second, all the gearbox TCs, both internal and external, were used. Third, only reliable gearbox TCs were used. Reliable gearbox TCs were defined as those locations where at least one of the redundant TCs remained bonded for the duration of the test and disassembly. Fourth, only gearbox housing TCs were used.

The bearing sensitivity study shows that the average absolute error between the model and test data is minimized when the vacuum bearing conductance correlations[4] are used. In fact, the match is slightly improved when the conductance is 10% greater, however for conservatism and simplicity the correlations[4] should be used. In an atmosphere, using a bearing conductance multiplier of 3 is shown to significantly improve model accuracy relative to the vacuum bearing conductance values. A multiplication factor of greater than 3 might be warranted, however the model improvement is marginal since average absolute error begins to asymptote. This calls into question whether this is a real effect, or a numerical coincidence. A multiplier of 3 applied to the vacuum correlations is judged to provide a conservative lower bounds estimate for bearing conductance in atmosphere.

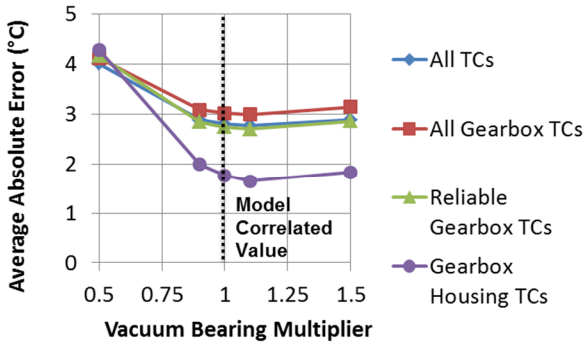

Figure 20: Model sensitivity to vacuum bearing conductance.

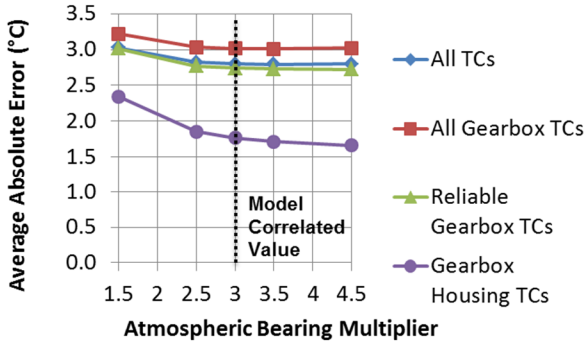

Figure 21: Model sensitivity to atmospheric bearing conductance.

5) Changes to gear-to-gear conductance

The assumed gear-to-gear contact conductance was based off an A/L of the gear-to-gear interface. This is an approximate term which was measured using the WSA-2 solids model using the method shown in Figure 19. Initially, the model for the test profile assumed k_{eff} = 0 W/m-K in a vacuum, and k_{eff} = 0.02 W/m-K in the low temperature N_2 cycles, k_{eff} = 0.025 W/m-K in the high temperature N_2 cycles, and k_{eff} = 0.015 W/m-K in the high temperature CO_2 cycles. These numbers were chosen based off the temperature dependent thermal conductivity of the gas during each part of the test.

Gear-to-gear conductance is not as well understood as bearing conductance. Unlike bearing conductance, the authors know of no previous efforts to estimate gear-to-gear contact conductance. Although it is clear, based on these test results, that gear-to-gear conductance is relevant in both a vacuum as well as in a gaseous environment, it is not clear exactly how strong the thermal conductance is. As a result, for the WSA-2 actuator, it is necessary to account for this conductance in a conservative manner.

Based on the test data, it is conservative to assume an effective grease conductance of 0.02 W/m-K. This conductance corresponds to a 13% grease coverage fraction with Braycote 601 since its conductivity is 0.15 W/m-K at a temperature of -35 °C[5]. It is also safe to assume that the effect of gear-to-gear gas conduction also contributes when an atmosphere is present, bringing the total effective conductance to somewhere between 0.03 and 0.045 W/m-K, depending on the gas species and temperature. The final correlated model for the test profile assumed k_{eff} = 0.02 W/m-K in a vacuum, and k_{eff} = 0.04 W/m-K in the low temperature N_2 cycles, k_{eff} = 0.045 W/m-K in the high temperature N_2 cycles, and k_{eff} = 0.035 W/m-K in the high temperature CO_2 cycles. These numbers were chosen based off the temperature dependent thermal conductivity of the gas during each part of the test. For an actuator on Mars, the low temperature CO_2 could result in an effective thermal conductivity as low as k_{eff} = 0.03 W/m-K, since the thermal conductivity of CO_2 is as low as 0.01 W/m-K. at -60 °C.

Both inspection of the gear to gear geometry and test data indicate that the conductance may be considerably higher, although we cannot say for sure. The A/L assumed in the calculation of conductance is a worst case since the L is the maximum gap between gears and the actual gap is much smaller in some areas (see Figure 19). This is discussed in more detail in the following paragraphs. However, it should be noted that using the A/L method given by Figure 19 along with a 13% grease area fraction and accounting for gas conduction is an improvement over the MSL approach, which was to completely neglect gear-to-gear conduction.

Similar to the sensitivity study for bearing conductance, a sensitivity study on gear-to-gear conductance was also performed. The effective thermal conductivity of the gear-to-gear interface was changed over a range of possible values. First, the effective thermal conductivity was changed during the vacuum portion of the test, leaving all other parts of the model constant, as shown in Figure 22. Next, the effective thermal conductivity was changed over a range of possible values during the atmospheric portion of the test, leaving all other parts of the model constant, as shown in Figure 23. The average absolute error between the model and the test data is used to understand how these changes affect model accuracy using four groups of TCs. First, all the actuator TCs were used. Second, all the gearbox TCs, both internal and external, were used. Third, only reliable gearbox TCs were used. Reliable gearbox TCs were defined as those locations where at least one of the redundant TCs remained bonded for the duration of the test and disassembly. Fourth, only gearbox housing TCs were used.

The gear-to-gear effective conductivity sensitivity study shows that the average absolute error between the model and test data is reduced when the gear-to-gear conduction is taken into account. In a vacuum, the average error on the gearbox housing TCs is minimized for k_{eff} = 0.02 W/m-K, even though the average absolute error of the gearbox and actuator TCs overall continues to decrease with increased gear-to-gear conduction. This justifies using k_{eff} = 0.02 W/m-K as a lower bound value for gear-to-gear grease conduction in a vacuum and corresponds to a 13% grease coverage fraction since Braycote 601 conductivity is 0.15 W/m-K at a temperature of -35 °C[5]. In the low temperature N_2 atmosphere, the average absolute error continues to decrease with increased gear-to-gear condition, but only marginally after k_{eff} = 0.1 W/m-K. This suggests that gear-to-gear gas conduction is surely taking place in addition to the grease conduction, but the extent of the gear-to-gear gas conduction is difficult to determine. As a result, adding the effective grease conductivity and temperature dependent gas conductivity serves as a conservative and physically meaningful way to account for gas conduction.

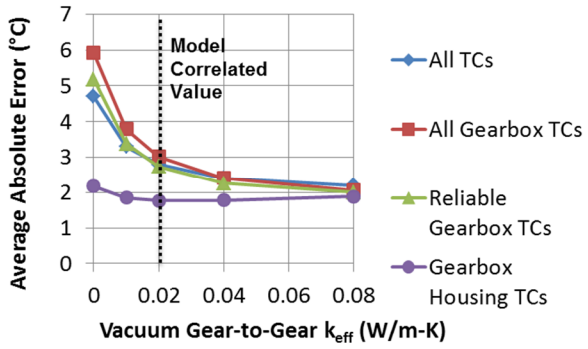

Figure 22: Model sensitivity to Vacuum Gear-to-Gear Effective Thermal Conductivity.

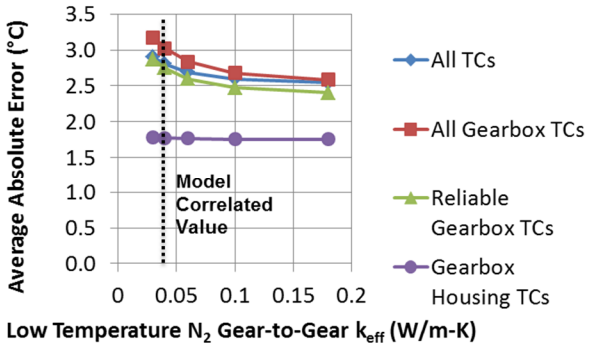

Figure 23: Model sensitivity to Low Temperature N_2 Gear-to-Gear Effective Thermal Conductivity.

Assuming a 13% grease area fraction with effective thermal conductance of 0.02 W/m-K, and then accounting for gas conduction on top of that is further justified by a second sensitivity study. In this study, the effective gear-to-gear conductivity (k_{eff}) was held constant over the entire test profile and varied from k_{eff} = 0 to 0.08 W/m-K. These model predictions were compared to the measured test data. The main point of this exercise was to have a way to visually examine the resulting temperature trends. This was done for all the internal temperature measurements, but only the 3rd Stage Sun Gear temperatures are shown in Figure 24 for brevity.

This plot, and others like it, verify that the model predicted sun, planet, and carrier temperatures are generally cooler than the measured test data. This suggests that the model remains conservative. In addition, it is clear that the effect of increasing gear-to-gear conductance begins to asymptotically decrease after about 0.02 W/m-K effective conductivity, which is why the author is hesitant to use a larger effective conductivity in the WSA-2 thermal model.

It should be emphasized that even though an effective grease conductivity of 0.02 W/m-K is still somewhat conservative, accounting for this level of gear-to-gear grease conduction helps to decrease warm up times. With the combination of grease and gas conduction, the effective conductivity can rise to k_{eff} ~ 0.035 W/m-K on Mars.

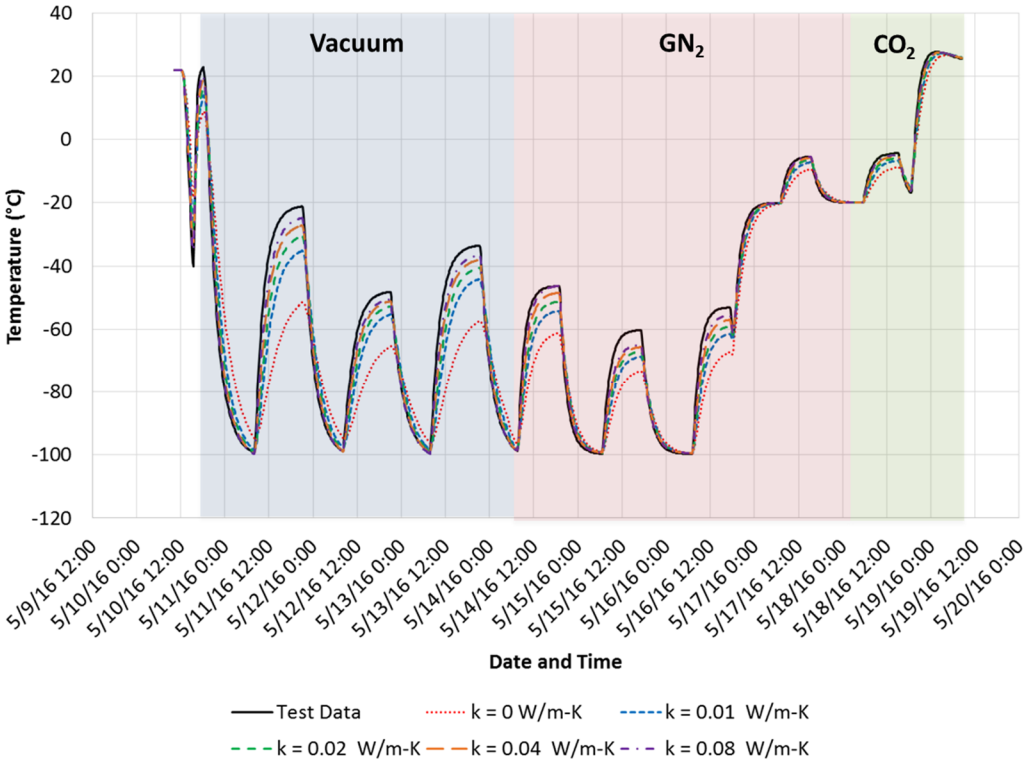

Figure 24: 3rd Stage Sun Gear-to-Gear Sensitivity Study.

C. Correlated Model

The final correlated model includes all the changes described previously. Figure 25 is a comparison of the measured test data to the initial and final correlated model predictions for the 3rd stage sun gear. Similar curves were produced for other measurement locations but only this curve is shown here for brevity. The figure shows that the correlated thermal model is much improved over the initial thermal model. Accounting for the gear-to-gear contact reduces the thermal gradients between the internal actuator components and the actuator housing, while remaining conservative.

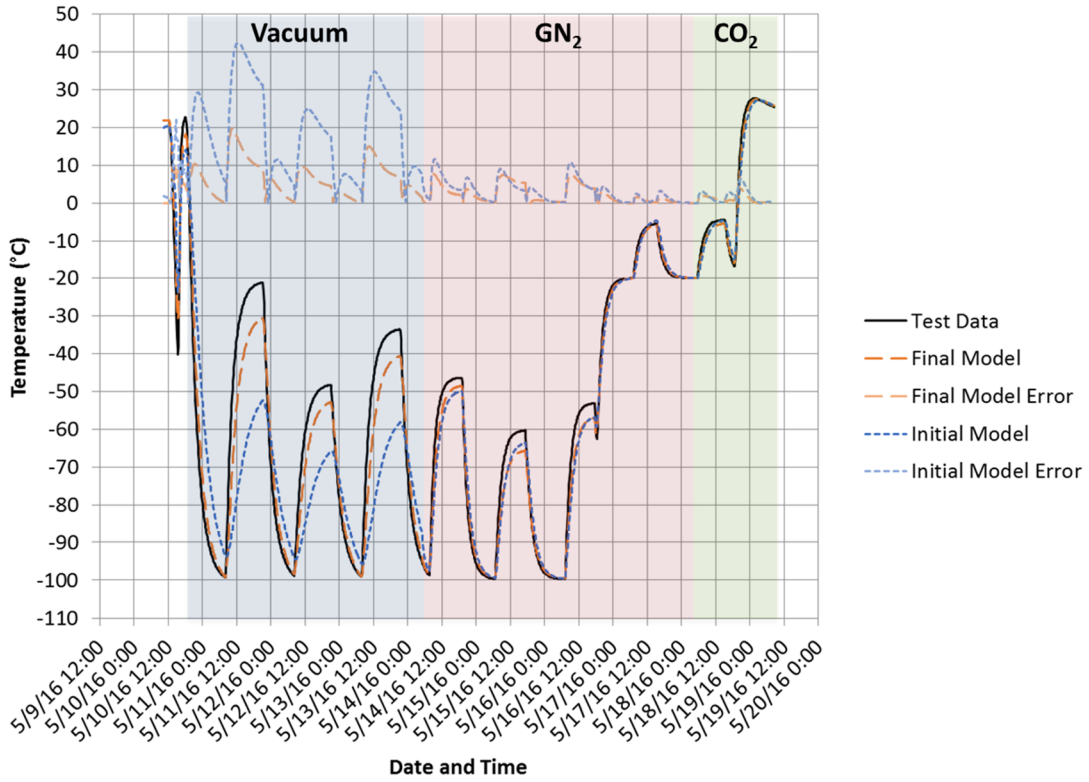

Figure 25: Comparison of 3rd Stage Sun Gear measured test data to initial and final model predictions.

IX. Lessons Learned

- This test was made possible by using 36 gage Type E TCs with PTFE insulation to instrument the actuator internals. There is simply no way that thicker wires would have fit in the tight tolerances inside the actuator.
- Careful planning was required to determine where there was sufficient clearance between internal actuator components. TCs were desired in some locations which simply did not have enough clearance for TCs to fit. As a result of careful planning of TC bead locations and TC wire routing, we were able to assemble the instrumented actuator on our first try.
- Practicing TC bonding was essential. TCs were bonded using a syringe and small bead of epoxy. Measurements of epoxy bead heights showed that bead sizes generally ranged from 1 to 2 mm (0.040" to 0.080") in height.
- During the actuator instrumentation process, a handheld DAQ was used to check the functionality of bonded TCs. To expedite the process, two wires with alligator clips were attached to the DAQ ports. This allowed aliveness tests to be performed quickly on the TCs, however it also introduced additional thermocouple junctions which skewed the temperature readings.
- Careful attention should be given to GSE and fit checks. Nearly all the oversights and challenges on this test were related to GSE.
- Bolted joints should always be torqued to the proper torque value. Some unusual results for the thermal profile of the encoder may have been caused by improperly torqued bolts.
- Heaters with tabs should have the tabs co-planar with the heating elements. The inlet (flange) heater, shown previously in Figure 7, has tabs which are mounted on a surface 90° from the main heater surface. This heater proved very difficult to install. This was a flight design which also was difficult to install on the MSL project. In the future, heaters should have tabs which are co-planar with the heating elements.
- Having TCs on the shroud and heat exchanger inlet lines is useful, especially if CO_2 testing is planned. The placement of TCs on the inlet lines provided knowledge of the coldest point inside the vacuum chamber, so that CO_2 gas could be used in the chamber without changing from gas to solid phase.
- When using contactors in Thermal Desktop®, care needs to be taken not to create artificial thermal shorts. This is one of the main errors which were fixed during model correlation.

- Epoxy bonding bolted interfaces that need to be disassembled again should be avoided. The breaking of the input and output housing bond likely caused many TCs to de-bond during disassembly. The epoxy was likely irrelevant for this thermal test due to the large number of bolts at the joint.
- Gravity effects on the internal conductances in actuators seem to be insignificant. The preloads in the actuator bearings are much higher than the body force due to gravity.

X. Conclusion

This test was a success and all test objectives were met. The test resulted in transient and steady thermal data for the WSA-2 actuator which was subsequently used to correlate a simplified thermal model. In addition, insight was gained into the bearing conductance and gear-to-gear conductance present inside the actuator. This insight will be applied to both the WSA-2 thermal model, as well as other thermal mechanism models. The average absolute error of all test data for the duration of the test was improved from 5.8 °C to 2.8 °C as a result of this model correlation. Bearing conductance values in a vacuum were estimated using published correlations[4], which have been verified to produce a good fit between the model and the test data. Bearing conductance values in a gaseous atmosphere use the same correlations, but with a multiplication factor of 3. Using this multiplication factor allowed the model to match the test data well, and should still be somewhat conservative since a survey of previous literature indicates that bearings have 3 to 10 times greater conductance in air than in a vacuum. The A/L for gear-to-gear conduction was estimated using the CAD geometry, where A is an approximate contact area and L is the maximum clearance between gear teeth. The effective gear-to-gear thermal conductivity of grease in vacuum is ~ 0.02 W/m-K, which corresponds to a ~ 13% grease coverage fraction. It is likely that the effective thermal conductivity of grease is higher than 0.02 W/m-K, however 0.02 W/m-K was used because it maintains some element of conservatism. When an atmosphere is present, gas conduction also acts to increase gear-to-gear conductance. The effective thermal conductivity of the gas conduction is dependent on the gas species and temperature. Accounting for gear-to-gear grease and gas conduction results in an improvement in model accuracy compared to the MSL approach which was to neglect this effect completely.

Acknowledgments

This research was carried out at the Jet Propulsion Laboratory, California Institute of Technology, under a contract with the National Aeronautics and Space Administration. The authors would like to thank the numerous individuals whose assistance was an essential part of the planning, preparation, and execution of this thermal test including, but not limited to Alex Bielawiec, Chris Wells-Weitzner, Carolyn Brennan, Andrew Kennett, Randy Lindemann, Ryan George, Rey Reyas, Pat Martin, Geoff Laugen, and Jackie Lyra. This work would not have been possible without your contributions to making this thermal test a reality. In addition, the author would like to thank Jen Miller and Gordy Cucullu for helpful discussions on the topic of thermal hardware. Reference herein to any specific commercial product, process, or service by trade name, trademark, manufacturer, or otherwise, does not constitute or imply its endorsement by the United States Government or the Jet Propulsion Laboratory, California Institute of Technology.

References

[1]Novak, K., Liu, Y., Lee, C.-J., and Hendricks, S., "Mars Science Laboratory Rover Actuator Thermal Design," *40th International Conference on Environmental Systems*, Barcelona, Spain, July 11-15, 2010.

[2]Stevens, K.T., and Todd, M.J., "Thermal Conductance Across Ball Bearings in Vacuum," Report No. *ESA-ESTL-25*, National Centre of Tribology, Risley, U.K., Feb. 1977, pp. 1-51.

[3]Takeuchi, Y.R., Dickey, J.T., Eby, M.A., and, Davis, S.E., "Thermal Conductance of Ball Bearings in Vacuum: A Review," *Journal of ASTM International*, Vol. 6, No. 1, 2008, pp. 1-12.

[4]Redmond, M., Novak, K., and Mireles, V., "Static Ball Bearing Thermal Conductance in Air and Vacuum: Review and Correlation," *AIAA Journal of Thermophysics and Heat Transfer* (accepted).

[5]Braycote® 601EF High Vacuum Grease, http://www.2spi.com/item/z05086/, retrieved on June 30, 2016.